

Search for new physics at HERA*

Valerie A. Noyes

Particle and Nuclear Physics Laboratory
University of Oxford, Oxford OX1 3RH, UK

Abstract

Recent results on the searches for new physics in ep collisions at HERA using the ZEUS and H1 detectors are presented. No evidence for excited fermions or supersymmetric particles within the context of the Minimal Supersymmetric Standard Model nor R-parity violation has been found using an integrated luminosity of up to 20 pb^{-1} . New limits have therefore been established.

Talk given at the Hadron Collider Physics conference, Stony Brook, June 1997, representing the ZEUS and H1 collaborations

1 Introduction

Due to the high centre of mass energy $\sqrt{s} = 300 \text{ GeV}$ and presence of a lepton and quark in the initial state, searches for physics beyond the standard model (SM) in ep collisions at HERA complement those made at LEP and the Tevatron. Indeed, much interest has focused on the recent results published by the ZEUS and H1 experiments [1] in which an excess of events above standard model predictions was reported in the previously unexplored region of high Q^2 . No attempt will be made in this review, however, to discuss this excess within the context of new physics. Further discussion and the latest results in the high Q^2 region can be found in the conference proceedings [2].

Preliminary results are presented on the search for excited fermions and selectron and squark production within the framework of R-parity conserving supersymmetric models using a total integrated luminosity of 9.3 pb^{-1} and 20 pb^{-1} respectively. Results on the search for R-parity violating squarks are

*OUNP-97-11

also discussed taking into account all possible R-parity violating and gauge decays and using an integrated luminosity of 2.83 pb^{-1} .

2 Search for excited fermions

The existence of excited leptons or quarks would provide compelling evidence for a new layer of fermion structure predicted within theories of compositeness. At HERA single excited electrons, quarks and neutrinos can in principle be produced with masses up to the kinematic limit of 300 GeV via the processes $ep \rightarrow f^*X, f^* \rightarrow fV$ shown in figure 1. The resonance is searched for via its electroweak decay to a light fermion, f , and a vector boson, V .

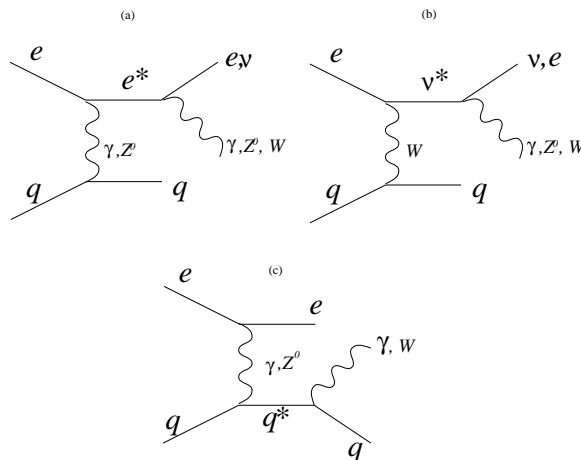


Figure 1: Feynman diagram for excited (a) electron, (b) neutrino and (c) quark production at HERA. Only the decay modes considered in this search are shown.

Direct searches for excited leptons and quarks have also been carried out at LEP and the Tevatron. In e^+e^- collisions, excited leptons may be pair or singly produced up to \sqrt{s} . At 95% confidence level (CL), any excited lepton ($e^*, \mu^*, \tau^*, \nu^*$) with mass below approximately 80 GeV has been ruled out [3]. This limit can be extended when the excited fermion is produced singly, however, becomes dependent on the coupling parameters at the ff^*V vertex as shown in figure 3. Experiments at the Tevatron have set stringent limits on the production of q^* in $p\bar{p}$ collisions at $\sqrt{s} = 1800 \text{ GeV}$, excluding q^* produced via the strong coupling [4] with masses between 80 and 760 GeV, except for a window between 570 and 580 GeV. HERA therefore extends the mass range over which e^* and ν^* can be searched and offers unique sensitivity for excited quarks produced via electroweak mechanisms.

In describing excited fermion production and decay it has become conventional to use the phenomenological model of Hagiwara et al [5], extended to include excited quark production by Baur et al [6]. The effective Lagrangian describing magnetic transitions from spin $\frac{1}{2}$ excited fermions f^* to ordinary fermions f has the form

$$L_{ff^*} = \frac{1}{\Lambda} \bar{f}^* \sigma^{\mu\nu} \left[g f \frac{\tau}{2} W_{\mu\nu} + g' f' \frac{Y}{2} B_{\mu\nu} + g_s f_s \frac{\lambda}{2} G_{\mu\nu} \right] f + h.c. \quad (1)$$

where Λ corresponds to the compositeness scale and the constants f , f' and f_s describe the effective changes from the standard model coupling constants g , g' and g_s . It is conventional to relate these unknown constants according to the chosen decay mode, thereby reducing the cross section dependence to a single parameter, f/Λ . For excited electron and excited quark searches $f = f'$ and $f_s = 0$ is chosen, exploring excited quark production via electroweak mechanisms. The radiative decay of excited neutrinos ($\nu_e^* \rightarrow \nu_e \gamma$) is only allowed when $f \neq f'$ and in this case $f = -f'$ and $f_s = 0$ is chosen.

The ZEUS search for excited fermions in positron-proton collisions uses an integrated luminosity of 9.4 pb^{-1} . The f^* decay modes which have been studied are shown in figure 1 and the subsequent decay channels of the heavy boson are listed in table 1. A detailed description of the analysis is given in [7].

f^*	Final states		
e^*	$e\gamma$	eZ^0 $\rightarrow eq\bar{q}$ $\rightarrow e\nu\bar{\nu}$	νW $\rightarrow \nu q\bar{q}$ $\rightarrow \nu e\nu$
ν^*	$\nu\gamma$	νZ^0 $\rightarrow \nu q\bar{q}$	eW $\rightarrow eq\bar{q}$ $\rightarrow ee\nu$
q^*	$q\gamma$	qW $\rightarrow qe\nu$	

Table 1: The decay modes and subsequent final states considered in this search for excited fermions.

Figure 2 shows the mass of the reconstructed $e\gamma$ final state in events with two isolated, high E_T electromagnetic clusters. The data are compared to the predicted Monte Carlo background, comprising mainly QED Compton and neutral current DIS events. The unshaded histogram shows the expected lineshape for an excited electron of mass 150 GeV. The cluster of four events

at masses around 135 GeV have features consistent with background expectations.

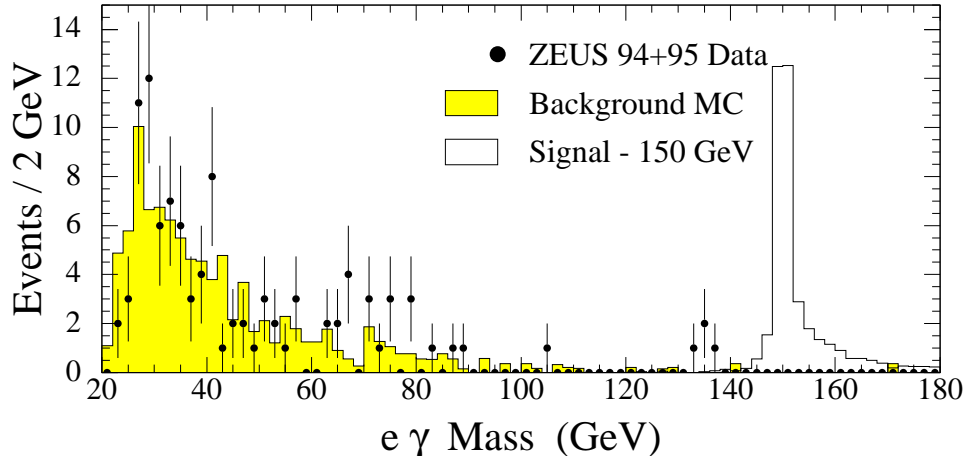


Figure 2: Distribution of the $e\gamma$ invariant mass for $e^* \rightarrow e\gamma$ candidates. The solid points show the ZEUS data from 1994 and 1995 while the shaded histogram represents the expected background. The unshaded histogram shows the expected distribution for a 150 GeV excited electron.

In the absence of a positive signal for excited leptons or quarks in any of the eight decay modes considered, upper limits on the characteristic coupling f/Λ as a function of the excited fermion mass were determined at 95% confidence level. Figure 3 shows the limits for e^* , ν^* and q^* production derived from each of the final states considered and from their combination using the assumptions about the couplings discussed previously. In each case the most stringent limits are derived from the $f^* \rightarrow f\gamma$ channel and dominate the combined limit from all three decay modes. The limits on e^* and ν^* production from the LEP experiments are also shown and demonstrate that HERA extends the limits for f^* production well beyond the ~ 170 GeV limits currently achieved at LEP.

Also shown on the ν_e^* plot is the limit from the previous search by ZEUS in e^-p collisions with a much lower integrated luminosity (0.55 pb^{-1}). This previous limit is more stringent for excited neutrino masses greater than 130 GeV because the ν_e^* production cross section in e^+p collisions is heavily suppressed relative to e^-p collisions, out-weighting the increase in integrated luminosity taken with positrons. High luminosity running with an e^- beam

planned for the 1998 run-period will substantially improve this limit.

Exclusion limits on the excited fermion masses can be determined by further assuming that $f/\Lambda = 1/M_{f^*}$. For this case, at 95% CL, excited electrons are ruled out in the mass range between 30 and 200 GeV using the combined limit from all three decay modes. Excited neutrinos with masses in the range 40 to 96 GeV are excluded while excited quarks with electroweak-only couplings are excluded over the range 40 to 196 GeV.

3 Search for selectrons and squarks

Supersymmetry (SUSY) is presently considered to be a promising candidate for a theory beyond the standard model. While there is strong theoretical motivation for its existence, there is currently no experimental evidence to support its prediction that each SM particle has a supersymmetric partner differing by a half-unit of spin.

Within the minimal supersymmetric standard model (MSSM) it is assumed that R-parity is conserved. This implies that SUSY particles can only be produced in pairs and that the lightest SUSY particle (LSP), taken here to be the lightest neutralino χ_1^0 is stable and weakly interacting thereby escaping detection.

Existing limits from the LEP experiments at $\sqrt{s} = 161$ GeV exclude selectrons with mass less than ~ 80 GeV [8] and spartners to the light quarks with masses less than 45 GeV (LEP1) [9]. Although the experiments at the Tevatron set strong limits on squark masses, these are dependent on the gluino mass [10] and can only be related to the HERA results assuming additional relations motivated by Grand Unified Theories (GUT).

At HERA the dominant MSSM process is the production of a selectron and squark via t channel neutralino exchange $ep \rightarrow \tilde{e}\tilde{q}X$ as shown in figure 4. Although the \tilde{e} and \tilde{q} can decay into any lighter gaugino and their SM partners, the cleanest experimental signature involves both the $\tilde{e} \rightarrow e\chi_1^0$ and $\tilde{q} \rightarrow q\chi_1^0$ decays and is the one considered here. The final state topology consists therefore of an electron which is acoplanar to the hadronic system and missing momentum.

Limits from a earlier search using the H1 detector and an integrated luminosity of 6.4 pb^{-1} have been published in [11]. The current search by ZEUS uses an integrated luminosity of 20 pb^{-1} . No signal was observed and preliminary exclusion limits on $\tilde{e}\tilde{q}$ production were derived at 95% confidence level. The limits are interpreted as exclusion regions in MSSM parameter space. The quantities used are M_2 and M_1 , the mass parameters for the SU_2 and U_1 gauginos, the higgsino mass parameter μ , and $\tan\beta \equiv v_2/v_1$, the

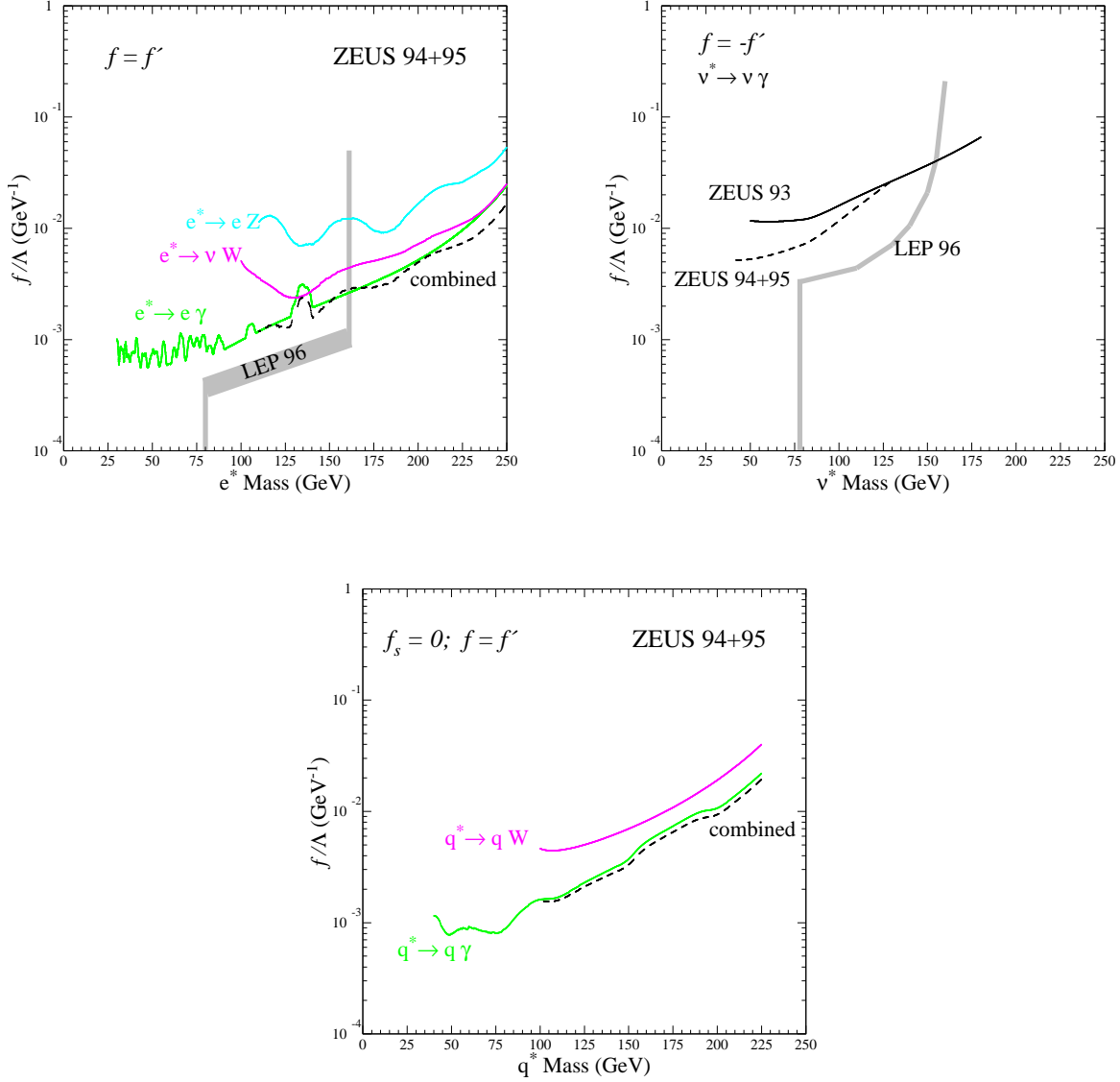


Figure 3: Limits on the characteristic coupling f/Λ as a function of the excited fermion mass for e^* , ν^* and q^* . The regions above the curves are excluded at 95% CL. Also shown are exclusion limits from LEP with centre-of-mass energies up to 161 GeV and the relationship between the couplings under which the limits were derived.

ratio of the two Higgs doublet vacuum expectation values.

Figure 5 shows the excluded region in the plane defined by the mass of the

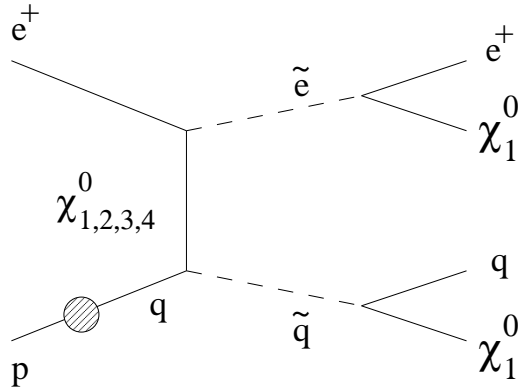


Figure 4: Selectron-squark production via neutralino exchange and the following decays to the LSP and SM partner.

lightest neutralino and half the sum of the selectron and squark masses for $\tan\beta = 1.41$ and different values of μ . For small values of μ ($\mu = -500$ GeV) and low neutralino masses, competing decays of the \tilde{e} and \tilde{q} to gauginos other than the χ_1^0 lead to reduced limits for $(M_{\tilde{e}} + M_{\tilde{q}})/2$. In the region $\mu = -50$ GeV, the branching ratios $B(\tilde{e} \rightarrow e\chi_1^0)$ and $B(\tilde{q} \rightarrow q\chi_1^0)$ are close to one because the other gauginos are heavier than $M_{\tilde{e}}$ or $M_{\tilde{q}}$. At large $M_{\chi_1^0}$ the mass difference between the \tilde{e} , \tilde{q} and χ_1^0 becomes small leading to a reduction in cross section together with a drop in detection efficiency limiting the upper exclusion bound. The excluded mass range extends to 72 GeV for $(M_{\tilde{e}} + M_{\tilde{q}})/2$ and 47 GeV for $M_{\chi_1^0}$, extending the previous limits set by H1 [11] with lower luminosity.

Figure 6 shows the excluded region in $M_{\tilde{e}}$ versus $M_{\tilde{q}}$ for different values of fixed χ_1^0 mass at $\mu = -500$ GeV. The limits are approximately functions of the sum $M_{\tilde{e}} + M_{\tilde{q}}$ due to the cross section and efficiency depending almost essentially on this sum. For $M_{\chi_1^0} = 40$ GeV squarks with masses between 55 GeV and 89 GeV are excluded for $M_{\tilde{e}} = 46$ GeV while selectrons with mass between 55 GeV and 92 GeV are excluded for $M_{\tilde{q}} = 46$ GeV. The selectron mass exclusion limits from LEP2 [8] are also indicated in figure 6 and show that the new HERA limits exclude a further region at high selectron and low squark masses.

In figure 7 the exclusion limits on M_2 versus μ are shown for $\tan\beta = 1.41$ and $M_2 = 2M_1$, a good approximation for the only SUSY GUT relation used here $M_1 = \frac{5}{3}M_2 \tan^2\theta_W$. For $\mu \ll 0$, the χ_1^0 is dominated by its photino component leading to couplings to the selectron and squark that are electromagnetic in strength and allow for a sizable cross section. As $\mu \sim 0$ the χ_1^0 becomes higgsino-like and the couplings and cross section become very

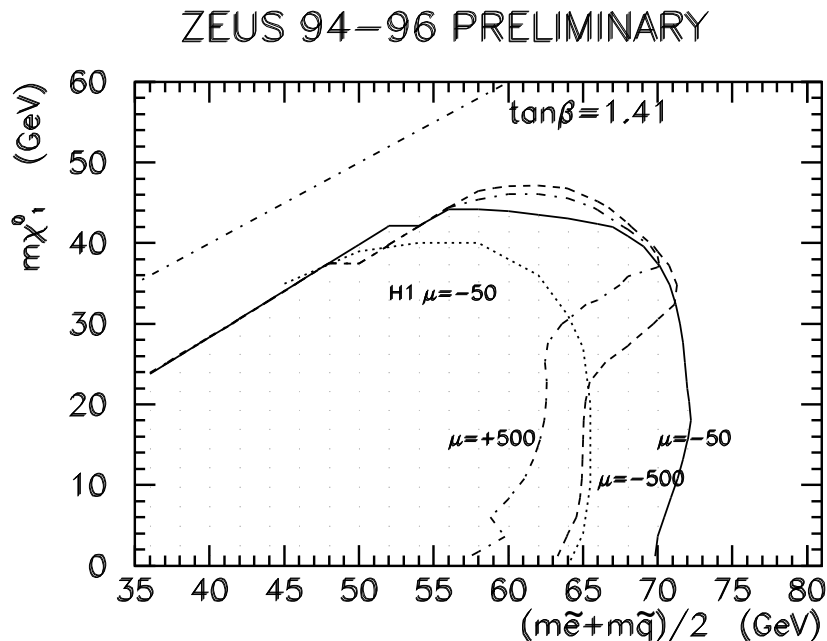


Figure 5: Regions excluded at 95% CL in the plane defined by the lightest neutralino mass and half the sum of the selectron and squark masses for $\mu=-500$ (dashed), -50 (full), $+500$ (dash-dotted line) and $\tan\beta = 1.41$. The limit from an earlier search by H1 is also shown for $\mu = -50$ GeV (dotted line).

small. The ZEUS limits are compared to those from chargino and neutralino searches at LEP [12] and extend considerably the limits on M_2 at negative μ .

4 Search for R-parity violating squarks

The search for R-parity violating squarks possessing a Yukawa coupling λ' to lepton-quark pairs is particularly promising at HERA. Such squarks can be singly produced as an s channel resonance up to the kinematic limit of $\sqrt{s} = 300$ GeV via positron-quark fusion. The squarks subsequently decay via their Yukawa coupling into fermions or via their gauge couplings into a quark and neutralino or a chargino as shown in figures 8(a), (c) and (b), (d) respectively. The χ_i^0 and χ_i^+ are mixed states of the supersymmetric partners to the SM gauge bosons and neutral Higgses and are in general unstable. In

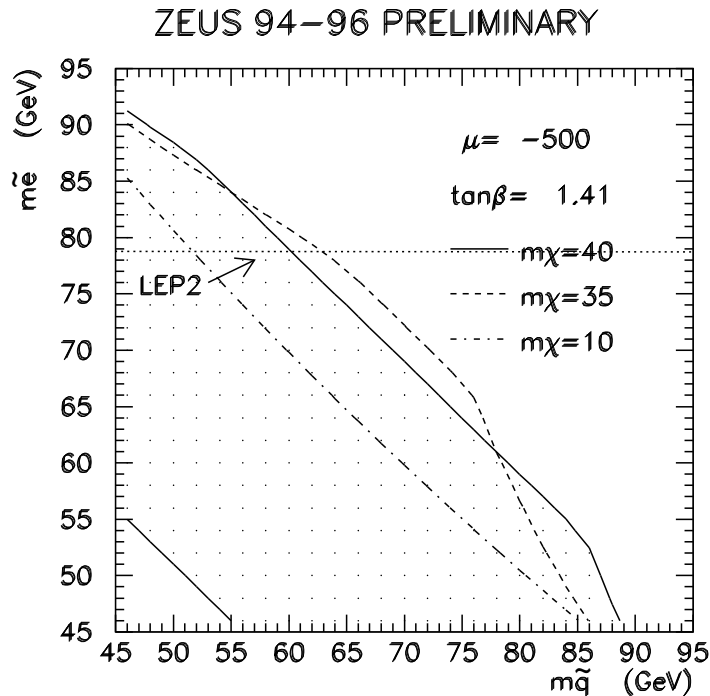


Figure 6: Regions excluded at 95% CL in the plane defined by the selectron and squark mass for fixed values of neutralino mass $M_{\chi_1^0} = 10$ (dash-dotted), 35 (dashed), 40 (full line) GeV and for $\mu = -500$ GeV and $\tan\beta = 1.41$. Selectron mass limits from LEP2 are also shown.

contrast to the MSSM, this also holds for the LSP which can decay into a quark, antiquark and lepton.

In the case where both the squark production and decay occur through a Yukawa λ'_{ijk} coupling¹ the final state signatures consist of a lepton and jet and are indistinguishable from standard neutral and charged current deep inelastic scattering on an event-by-event basis. The strategy then involves searching for a resonance at high mass ($M_{\tilde{q}} = \sqrt{xs}$) where x is the Bjorken scaling variable. No attempt is made here to interpret the recently reported excess of events at high x and Q^2 observed at the HERA experiments [1] within the context of R-parity violating SUSY.

Using an integrated luminosity of 2.8 pb^{-1} the squark mass is reconstructed using the e^+ energy and polar angle in the selected neutral current

¹the ijk indices correspond to the generations of superfields L_i , Q_j and \bar{D}_k containing the left-handed lepton doublet and quark doublet, and the right-handed quark singlet respectively

ZEUS 94–96 PRELIMINARY

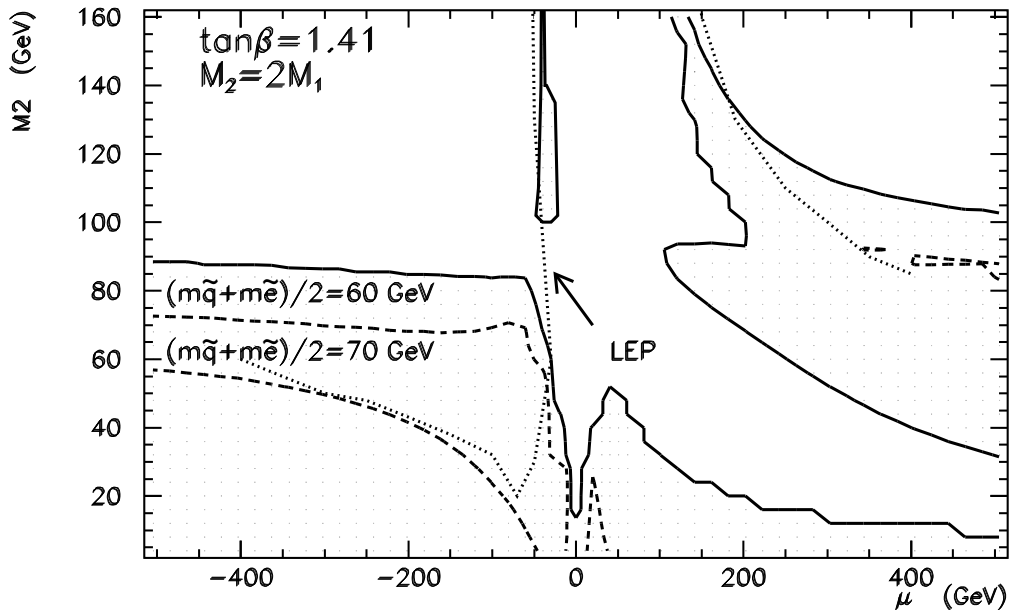


Figure 7: Region excluded at 95% CL in the plane defined by M_2 and μ for $M_{\tilde{e}} = M_{\tilde{q}} = 60$ (full) and 70 (dashed line) GeV for $\tan\beta = 1.41$. The area below the dotted line is excluded by LEP.

sample and the hadronic final state in the charge current sample. Figures 9(a) and (b) show the reconstructed mass for the neutral and charged current event samples respectively. The shaded histogram indicates the background Monte Carlo while the dashed histogram compares the mass distribution for a mixture of background and SUSY MC events for $M_{\tilde{q}} = 150$ GeV and $M_{\tilde{q}} = 75$ GeV respectively. No significant deviation from the number of expected events is observed when including all sources of systematic error.

Squark decays via gauge couplings $\tilde{u}_L \rightarrow u\chi_i^0$ or $d\chi_j^+$ and $\tilde{d}_R \rightarrow \bar{d}\chi_i^0$ have also been considered (figure 8 (b) and (d)). Furthermore, both gauge and R-parity violating decays of the chargino have been taken into account together with the dependence of the χ_1^0 decay on its gaugino-higgsino composition governed by the fundamental SUSY parameters. In particular if the χ_1^0 is dominated by its photino component it will tend to decay $\chi_1^0 \rightarrow e^\pm q\bar{q}$, giving the possibility of a “wrong sign” lepton (with respect to the charge of the incoming lepton beam) in the final state.

Six distinguishable event topologies are listed in table 2 and have been

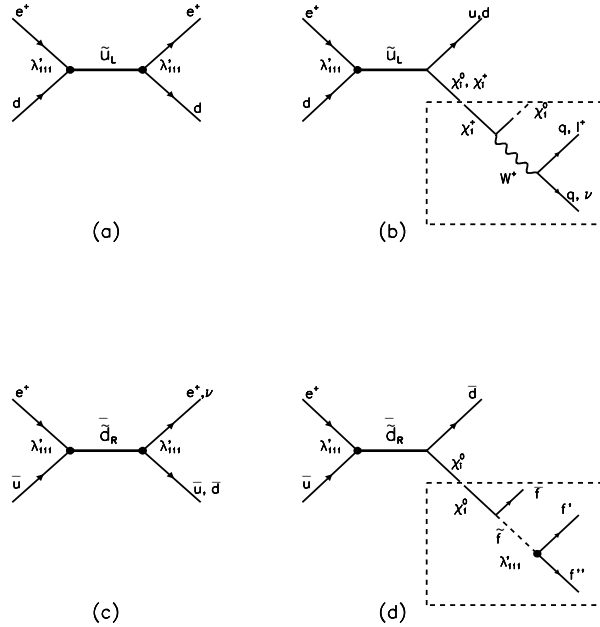


Figure 8: First generation R-parity violating squark production at HERA followed by (a), (c) R-parity violating decays and (b) and (d) gauge decays. In (b) and (d) the chargino and neutralino undergo subsequent R-parity violating decays.

considered in this search, full details of which are given in [13]. No significant excess of events was observed in any channel, however, an interesting event with a final state μ and jet passed the selection cuts for topology d in table 2 and is shown in figure 10. Detailed analysis of the event [14] shows the μ^+ has a $p_T = 23$ GeV and there is an overall missing $p_T = 18.7$ GeV, taking the p_T of the μ^+ into account. The dominant source of background is expected from single W^+ production followed by the decay $W^+ \rightarrow \mu^+ \nu X$. However the properties of this event are such that there is only a $\sim 3\%$ probability for such an interpretation and a negligible contribution from misidentified charged current DIS. A second similar candidate has been observed during 1997 data-taking and is shown in figure 11, however more data will be required to establish the origin of these events.

In the absence of a significant deviation from SM expectations, 95% confidence level limits on the Yukawa coupling λ'_{111} are derived as a function of squark mass combining all contributing channels. Figure 12 shows the lim-

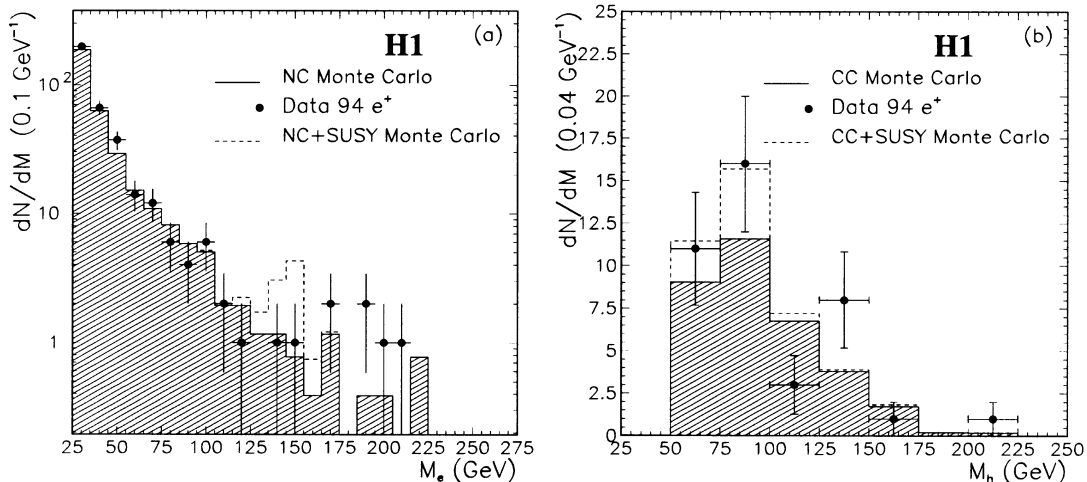


Figure 9: Reconstructed mass distribution in the (a) neutral and (b) charged current event samples using an integrated luminosity of 2.8 pb^{-1} . The shaded histogram shows the background MC spectrum while the dashed histogram indicates the mass distribution of a mixture of background MC and a SUSY signal with $M_{\tilde{q}} = 150 \text{ GeV}$ and $M_{\tilde{q}} = 75 \text{ GeV}$ in (a) and (b) respectively.

its assuming that the lightest neutralino is a pure photino and for different photino masses. First generation squarks with masses up to 240 GeV are excluded at 95% confidence level for coupling strengths $\lambda_{111}^2/4\pi > \alpha_{em}$, thereby extending the limits inferred from the Tevatron di-lepton data [15].

From the analysis of the λ'_{111} case, limits on the λ'_{1jk} couplings can be deduced by folding in the proper parton densities. The results given in table 3 are for $M_{\tilde{q}} = 150 \text{ GeV}$ and $M_{\chi_1^0} = 80 \text{ GeV}$ for $\tilde{\gamma}$ -dominant and \tilde{Z} -dominant χ_1^0 . No other direct limits for λ'_{1jk} where j or $k \neq 1$ have been published.

5 Search for stop

The cases where $\lambda'_{131} \neq 0$ or $\lambda'_{131} \neq 0$ are of particular interest as they allow for the direct production of stop. A light stop mass eigenstate, \tilde{t}_1 , much lighter than the top quark or other squarks could exist. The search for such a stop mass eigenstate is extended towards lower masses by considering $\tilde{t}_1 \tilde{t}_1$ pair production via photon-gluon fusion as shown in figure 13. Here the \tilde{t}_1 is assumed to be lighter than the top quark and the lightest chargino so that the decays into $t\chi_1^0$ and $b\chi_1^+$ are forbidden so that the decay $\tilde{t}_1 \rightarrow e^+q$ will dominate.

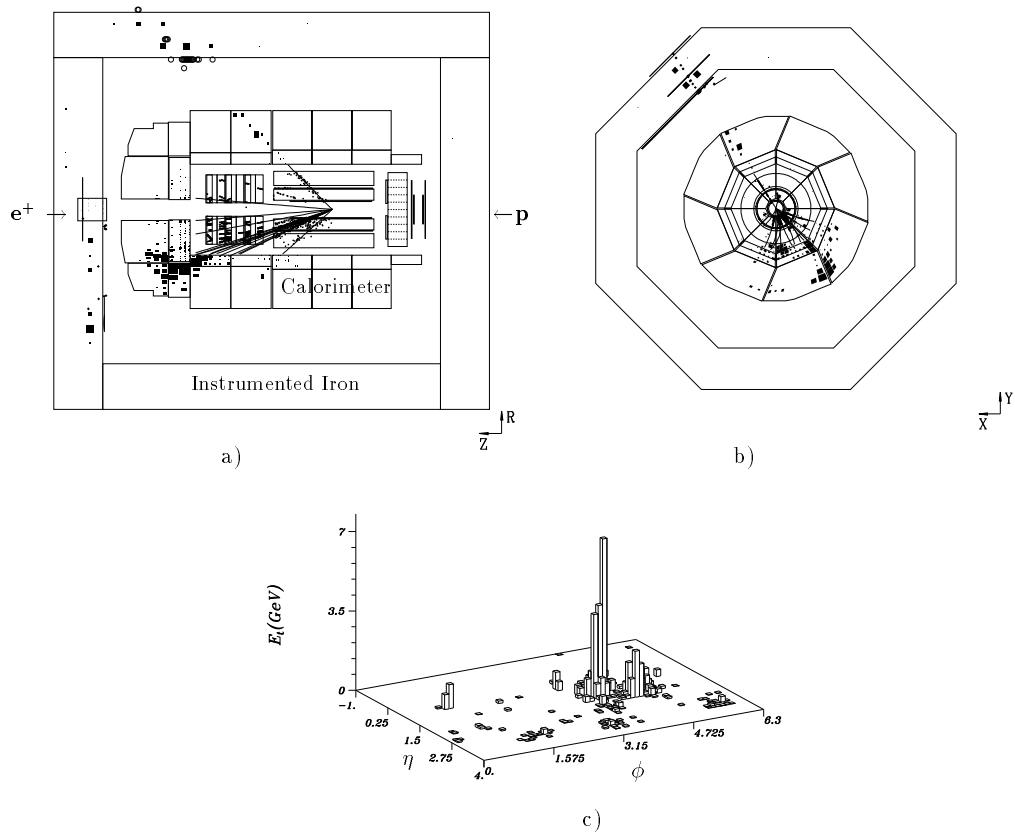


Figure 10: Display of the $e^+p \rightarrow \mu + jet$ candidate found using the H1 detector.



Run 186729 Event 702 Class: 2 4 8 20 22 24 26

Run Date 4/5/97

THE-2nd-EVENT

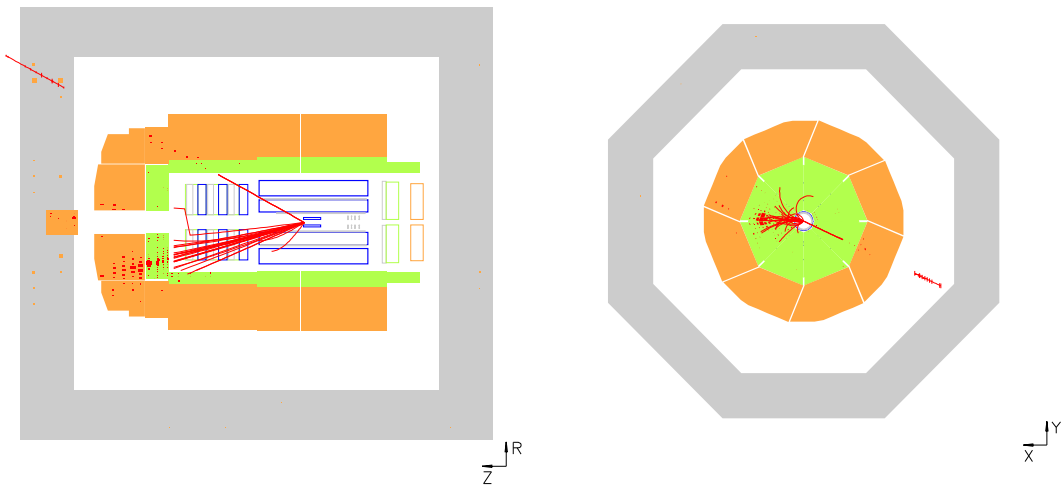


Figure 11: A second $e^+p \rightarrow \mu + jet$ candidate recently found at H1.

Topology	χ_1^0 nature	Decay process	Signature
a	$\tilde{\gamma}, \tilde{Z}$ $\tilde{\gamma}, \tilde{Z}, \tilde{H}$ $\tilde{\gamma}, \tilde{Z}$	$\tilde{q} \rightarrow q\chi_1^0 \rightarrow qe^+\bar{q}q$ $\tilde{u}_L \rightarrow d\chi_1^+ \rightarrow de^+d\bar{d}$ $\tilde{u}_L \rightarrow d\chi_1^+ \rightarrow W^+\chi_1^0$ $\rightarrow q\bar{q}e^+\bar{q}q$	High p_T e^+ + multiple jets
b	$\tilde{\gamma}, \tilde{Z}$ $\tilde{\gamma}, \tilde{Z}$	$\tilde{q} \rightarrow q\chi_1^0 \rightarrow qe^-\bar{q}q$ $\tilde{u}_L \rightarrow d\chi_1^+ \rightarrow W^+\chi_1^0$ $\rightarrow q\bar{q}e^-\bar{q}q$	High p_T e^- + multiple jets
c	$\tilde{\gamma}, \tilde{Z}$ $\tilde{\gamma}, \tilde{Z}$ $\tilde{\gamma}, \tilde{Z}, \tilde{H}$ \tilde{H}	$\tilde{q} \rightarrow q\chi_1^0 \rightarrow q\nu\bar{q}q$ $\tilde{u}_L \rightarrow d\chi_1^+ \rightarrow W^+\chi_1^0$ $\rightarrow q\bar{q}\nu\bar{q}q$ $\tilde{u}_L \rightarrow d\chi_1^+ \rightarrow d\nu u\bar{d}$ $\tilde{u}_L \rightarrow d\chi_1^+ \rightarrow W^+\chi_1^0$ $\rightarrow q\bar{q}\chi_1^0$	Missing p_T + multiple jets
d	\tilde{H}	$\tilde{u}_L \rightarrow d\chi_1^+ \rightarrow W^+\chi_1^0$ $\rightarrow l^+\nu\chi_1^0$	High p_T e^+ or μ^+ missing p_T + 1 jet
e	$\tilde{\gamma}, \tilde{Z}$	$\tilde{u}_L \rightarrow d\chi_1^+ \rightarrow W^+\chi_1^0$ $\rightarrow l^+\nu e^\pm\bar{q}q$	High p_T $e + e^+$ or μ^+ + missing p_T + multiple jets
f	$\tilde{\gamma}, \tilde{Z}$	$\tilde{u}_L \rightarrow d\chi_1^+ \rightarrow W^+\chi_1^0$ $\rightarrow l^+\nu\nu\bar{q}q$	High p_T e^+ or μ^+ + missing p_T + multiple jets

Table 2: Squark decay channels in R-parity violating SUSY classified according to distinguishable event topologies.

The final state for such a signature will comprise two isolated and acollinear high E_T electrons together with two high E_T jets and no missing momentum. Details of the analysis are published in [13]. As no signal was observed using $\int \mathcal{L} dt = 2.83 \text{ pb}^{-1}$, exclusion limits were derived at 95% CL, combining those channels from the previous search in which single \tilde{t}_1 is produced. Figure 14 shows the limits on the coupling $\lambda'_{131} \cos \theta_t$ as a function of $M_{\tilde{t}_1}$. The exclusion limits from the pair production analysis, indicated by the shaded area, are independent of the coupling and exclude masses between 9 and 24.4 GeV.

The region above the curve in figure 14 is excluded by the single stop

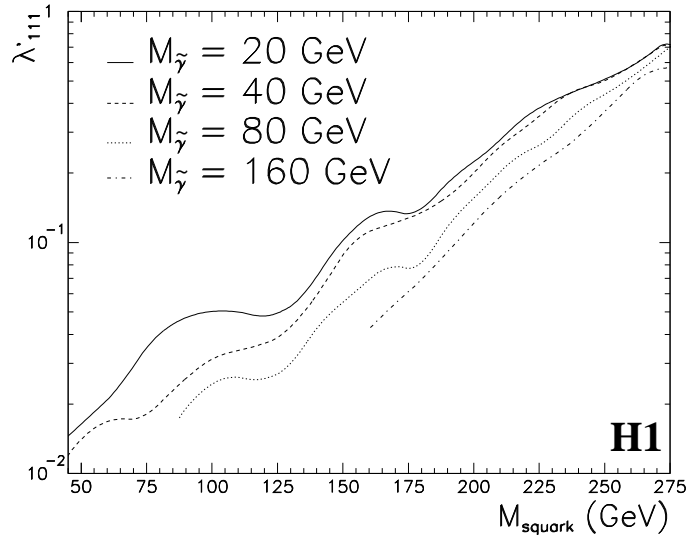


Figure 12: Exclusion limits for the squark coupling λ'_{111} as a function of squark mass for various fixed photino masses and taking $\tan\beta = 1$. The regions above the curves are excluded at 95% CL and combine R-parity violating and gauge decays of the squarks.

search. For coupling strengths $(\lambda'_{131} \cos\theta_t)^2/4\pi \geq 0.01\alpha_{em}$ stop masses below 138 GeV are excluded. In the region where the stop mass limits extend beyond the top mass, the limits are only valid when $M_{\tilde{t}_1} < M_{top} + M_{\chi_1^0}$.

6 Conclusions and future prospects

The ZEUS and H1 experiments have found no evidence for excited fermions or supersymmetry using an integrated luminosity of up to 20 pb^{-1} . Upper limits at 95% confidence level have been established on excited electron and neutrino production which are more stringent than the current limits at LEP. The limits on excited quark production via electroweak mechanisms complement those measurements made at the Tevatron where their strong production is explored. New limits on SUSY particle production at HERA have been established within the context of the MSSM and R-parity violating SUSY, including limits on stop production.

The future prospects for discovery at HERA continue to improve as the luminosity delivered by the HERA accelerator continues to increase. In 1997 each experiment expects to collect an integrated luminosity of $\sim 30 \text{ pb}^{-1}$

λ'_{1jk}	production processes	$\tilde{\gamma}$ -like χ_1^0	\tilde{Z} -like χ_1^0
λ'_{111}	$e^+ + \bar{u} \rightarrow \tilde{d}_R$ $e^+ + d \rightarrow \tilde{u}_L$	0.056	0.048
λ'_{112}	$e^+ + \bar{u} \rightarrow \tilde{s}_R$ $e^+ + s \rightarrow \tilde{u}_L$	0.14	0.12
λ'_{113}	$e^+ + \bar{u} \rightarrow \tilde{b}_R$ $e^+ + b \rightarrow \tilde{u}_L$	0.18	0.15
λ'_{121}	$e^+ + \bar{c} \rightarrow \tilde{d}_R$ $e^+ + d \rightarrow \tilde{c}_L$	0.058	0.048
λ'_{122}	$e^+ + \bar{c} \rightarrow \tilde{s}_R$ $e^+ + s \rightarrow \tilde{c}_L$	0.19	0.16
λ'_{123}	$e^+ + \bar{c} \rightarrow \tilde{b}_R$ $e^+ + b \rightarrow \tilde{c}_L$	0.30	0.26
λ'_{131}	$e^+ + \bar{t} \rightarrow \tilde{d}_R$ $e^+ + d \rightarrow \tilde{t}_L$	0.06	0.05
λ'_{132}	$e^+ + \bar{t} \rightarrow \tilde{s}_R$ $e^+ + s \rightarrow \tilde{t}_L$	0.22	0.19
λ'_{133}	$e^+ + \bar{t} \rightarrow \tilde{b}_R$ $e^+ + b \rightarrow \tilde{t}_L$	0.55	0.48

Table 3: Upper 95% CL exclusion limits on the couplings λ'_{1jk} for $M_{\tilde{q}} = 150$ GeV and $M_{\chi_1^0} = 80$ GeV.

of e^+p collision data, doubling the total data sample collected pre-1997. In 1998-99 HERA will operate with an e^- beam and the goal is to deliver $\int \mathcal{L} dt = 50 \text{ pb}^{-1}$ per experiment, thereby improving the sensitivity for the search for excited neutrinos, certain leptoquarks and R-parity violating squarks. HERA will undergo a major luminosity upgrade in the shutdown between 1999-2000, beyond which each experiment expects to collect a total of 1000 pb^{-1} .

References

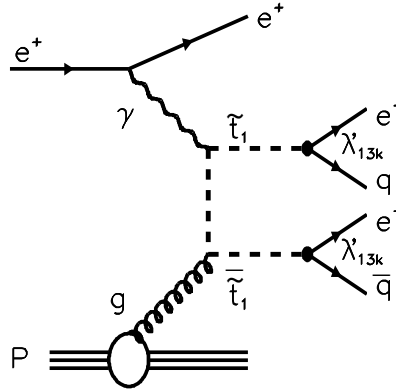


Figure 13: Stop pair production via photon-gluon fusion followed by the subsequent R-parity violating decay $\tilde{t}_1 \rightarrow eq$.

- [1] ZEUS Collaboration, J. Breitweg et al., Z. Phys. C74 (1997) 207;
H1 Collaboration, C. Adloff et al, Z. Phys. C74 (1997) 191.
- [2] Transparencies shown by J. Meyer (H1), D.C. Williams (ZEUS) and
D.K. Krakauer are available from
<http://sbhep1.physics.sunysb.edu/~hadrons/program.html>
- [3] OPAL Collaboration, K. Ackerstaff et al., Phys. Lett. B391 (1997) 197;
DELPHI Collaboration, P. Abreu et al., Phys. Lett. B393 (1997) 245;
L3 Collaboration, M. Acciarri et al., Phys. Lett B401 (1997) 139.
- [4] CDF Collaboration, F. Abe et al., Phys. Rev Lett 74 (1995) 3538;
CDF Collaboration, F. Abe et al., Phys. Rev. D55 (1997) 5263.
- [5] K. Hagiwara, S. Komamiya and D. Zeppenfeld, Z. Phys. C29 (1985) 115.
- [6] U. Baur, M. Spira and P.M. Zerwas, Phys. Rev D42 (1990) 815.
- [7] ZEUS Collaboration, J. Breitweg et al., DESY-97-112, June 1997.
- [8] OPAL Collaboration, K. Ackerstaff et al., Phys. Lett. B396 (1997) 301.
- [9] OPAL Collaboration, M.Z. Akrawy et al., Phys. Lett. B240 (1990) 261;
DELPHI Collaboration, P. Abreu et al., Phys. Lett. B247 (1990) 148;
ALEPH Collaboration, D. Decamp et al., Phys. Rep. 216 (1992) 253.

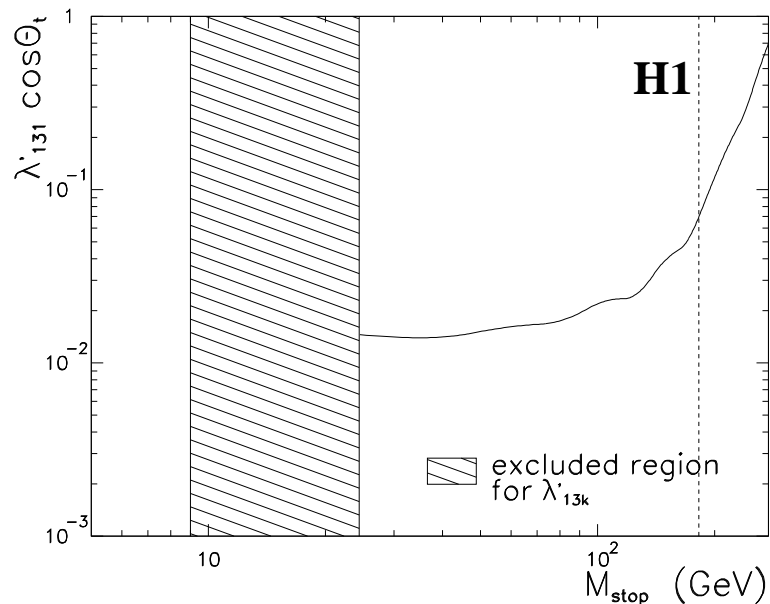


Figure 14: Exclusion limits on the coupling $\lambda'_{131} \cos \theta_t$ as a function of the stop mass derived at 95% CL. The shaded area is excluded from the pair-production search while the region above the curve is excluded from single stop production.

- [10] D0 Collaboration, S. Abachi et al., Phys. Rev Lett 75 (1995) 618;
CDF Collaboration F. Abe et al, Phys. Lett. 76 (1996) 2006.
- [11] H1 Collaboration, S. Aid et al., Phys. Lett. B380 (1996) 461.
- [12] ALEPH Collaboration, D. Buskulic et al., Z. Phys. C72 (1996) 549.
- [13] H1 Collaboration, S. Aid et al., Z. Phys. C71 (1996) 211.
- [14] H1 Collaboration, T. Ahmed et al., DESY 94-248 (December 1994)
- [15] D.P. Roy, Phys. Lett. B283 (1992) 270.